Temporal and Spatial Changes of Water Occurrence in the Selenga River Delta

Saeid Aminjafari[1], Ian Brown[1], Sergey Chalov[2], Marc Simard[3], Jerker Jarsjö[1], Mehdi Darvishi[1], Fernando Jaramillo[1,4]

[1]Department of Physical Geography and Bolin Centre for Climate Research, Stockholm University, SE–106 91, Stockholm, Sweden.

[2]Faculty of Geography, Lomonosov Moscow State University, 119991 Moscow, Russia.

[3]Radar Science and Engineering Section, NASA Jet Propulsion Laboratory, USA.

[4]Baltic Sea Centre and Stockholm Resilience Center, Stockholm University, SE-106 91 Stockholm. Sweden.

Corresponding author: Saeid Aminjafari (saeed.aminjafari@natgeo.su.se)

Key Points:

- Water occurrence has decreased in the Selenga River Delta within the last three decades.
- The change in water occurrence correlates with the change in the river discharge, and not with the change in lake water level.
- The Change in river discharge and sediment discharge are changing the stream network of the Selenga River Delta.

Abstract

Surface water occurrence in river deltas is governed by precipitation, evaporation, and the influx and outflux of water to and from the delta. Although studies of changes in water occurrence have been conducted at large scales, precise detection of changes in water occurrence is missing for most important river deltas. We take the case of the endorheic Selenga River Delta in Russia and train an accurate classification and quantification of water occurrence in its domain. We utilize remotely sensed observations of the Landsat satellite imagery during the last 33 years and implement supervised classification to map the surface water extent and its changes between periods of 1987-2002 and 2003-2019. We find that water occurrence has decreased in the Delta, with seasonally inundated areas presenting more pronounced decreases in water occurrence than permanent water bodies. We show that the change in the surface runoff is the main driver of changes in the spatial patterns of surface water with $R^2 = 0.58$, while changes in water level in the recipient Lake Baikal do not influence water occurrence in the Delta. Our results show that the shrinkage and expansion of the water surface reflect the change in the freshwater supply of the Delta, and the management of the Selenga River needs to consider the impact of changes on the water occurrence.

1 Introduction

River deltas are responsible for ecosystem services to humans such as freshwater storage, pollutant retention and attenuation, recreational activities, flood control, and fishing (Golden et al., 2014; Guo et al., 2017; Lu & Kwoun, 2008). Despite their importance in providing these services, they are now under pressure by effects from human development and greenhouse-gas emission climate change. For instance, in-stream quarrying leads to sediment compaction due to the extraction of the resources beneath the sediments. Upstream water impoundment and regulation decreases sediment discharge and flattens runoff peaks necessary for hydraulic flushing and wetland sheet flow (Syvitski et al., 2009). Change in water occurrence is an indicator of such effects (Zhang et al., 2017). The term water occurrence is defined as the presence of water on the specific location on the surface and in a particular moment in time. For the particular case of deltas, water occurrence can be permanent in areas of open water such as main river channels, streams, and in-stream wetlands, or temporary such as sand banks, flooded wetlands and flood plains. Apart from the direct effects from human activities, changes in water

occurrence are also driven by in-stream hydraulics, fluvial geomorphologic processes and sediment transport. The study of the changes in hydrological connectivity resulting from the spatial and temporal distribution of water occurrence and the distribution of surface water patches in the deltas are relevant for conservation of deltaic ecosystems and agricultural-industrial activities (Cui et al., 2020; Nguyen et al., 2020), management of these water resources and to strengthen their resilience to climatic and human-driven impacts and their functions as biodiversity niches and ecosystem service providers (Borja et al., 2020).

Concerning the changes in the hydrology and morphology of the deltas irrespective of the changes' direction, global estimations point to gains of roughly 54 square kilometers of land per year due to land-use change and deforestation (Nienhuis et al., 2020). On the other hand, during the last two decades, floods caused by heavy precipitation, river overflow, and storm surges have submerged 260,000 km^2 in 85 percent of all deltas around the world (Syvitski et al., 2009). Although these studies agree on the global expansion of the water surface, the magnitude of the change depends on whether they have studied the seasonal and permanent water bodies separately or together (Borja et al., 2020; Donchyts et al., 2016; Pekel et al., 2016). The change in global surface water occurrence is spatially heterogeneous and its direction of change, loss or gain, varies among deltas (Borja et al., 2020). For example, Zhang et al. (2017) detected 99 newly formed lakes and increased lake areas on the Tibetan Plateau from 1970 to 2013, as opposed to what was found in the neighboring Mongolian Plateau during the same period where 208 lakes vanished and in 75% of the remaining lakes (Zhang et al., 2017). The studies attempting to quantify changes in water occurrence at the global scale, although are very relevant for the assessment of global water resources, lack a detailed understanding of local changes in water occurrence, obviously pertaining the scale of the global scale of such assessments. They also fail to recognize the main drivers of changes in water occurrence in each water resource, mainly if these are climatic (i.e., changes in evaporation, runoff, sea level rise) or anthropogenic (in-stream mining, drainage, infrastructure).

Giesen (2020) and Neinhuis et al. (2020) emphasize that regional focus on both small and larger and more complex deltas such as the Niger, Huang He, Mekong, and the Ganges is necessary to understand and manage the hydrological and morphological changes in deltas with greater global impacts. They also justify the importance of local studies that aim to identify changes in water

occurrence in individual case studies of regionally important deltas providing a large set of ecosystem services.

Furthermore, satellite observations and machine learning algorithms are usually used to understand water occurrence and its changes (Allen & Pavelsky, 2018; Borja et al., 2020; Chini et al., 2017; Donchyts et al., 2016; Guo et al., 2017; Pekel et al., 2016; Zhang et al., 2017). The Landsat project, with more than 35 years of high-resolution acquisitions is a convenient source of optical imagery to monitor change in water occurrence, with even several images available per month for specific deltas. Advanced computational algorithms and cloud-based platforms enable the processing of large amounts of data in relatively short periods, providing a high-spatial resolution of changes in water occurrence. Unsupervised classification methodologies are usually used to study long-term changes in global water occurrence (Borja et al., 2020; Donchyts et al., 2016; Pekel et al., 2016), mostly without training data. Training data, or in other words using pre-existing knowledge in the spatial distribution of water occurrence, would greatly improve the prediction of water occurrence, and avoid misclassifications of water surfaces, as it sometimes occurs with unsupervised classification methodologies.

We here use the case of the Selenga River Delta to address the three knowledge gaps mentioned; 1) to study changes in water occurrence with focus on deltas, 2) identifying the contribution of hydroclimatic drivers to changes in water occurrence, and 3) applying training data to improve the accuracy of the water-land delineation required to determine water occurrence. We apply this method in the Selenga River Delta in Russia, an endorreic delta covering 540 km^2 and a water resource that plays a key role in the ecosystem of the region and of Lake Baikal, the inland water body receiving its waters. The delta has been experiencing a decrease in size that goes against the global expansion of other water bodies (Borja et al., 2020; Donchyts et al., 2016; Pekel et al., 2016).

2 Materials and Methods

2.1 Study area

The Selenga River Delta is located in eastern Russia (Figure 1) along the southern shore of Lake Baikal. Lake Baikal is the oldest (25 million years) and the deepest (~1800 meters) lake in the world and a World Natural Heritage Site (UNESCO 1997). Lake Baikal contains

approximately 20% of all liquid fresh water on Earth (Berhane et al., 2018; Borisova, 2019). The Selenga River is the main river flowing into Lake Baikal; one of around 365 other rivers. It is responsible for almost 50% of the runoff water and 60% of the transported sediments into the lake system, and its hydrological basin covers more than 82% of the Lake's basin (Berhane et al., 2018). The unique habitats and ecosystem of the Selenga River Delta on Lake Baikal and its purifying function have made this Delta a Ramsar wetland of international importance (Berhane et al., 2018; Lane et al., 2015). The fan-shaped herbaceous wetland of the Selenga River Delta covers an area of roughly 540 km^2 and receives mean annual precipitation of 315 mm (Figure 2b), concentrated from April to October and causing floods and freshets in the main channel and tributaries, as reflected in the values of monthly runoff (Figure 2a). The arid continental climate is described by temperature variations between +14°C on average in July and -19°C in January permits a growing season of 140 to 150 days that starts in mid-May (Figure 2c), (Berhane et al., 2018; Lane et al., 2015). Although the highest temperatures occur during the summer, the biggest monthly temperature differences occur in the winter (bigger boxes and higher differences between maximum and minimum).

The river faces several socioeconomic and environmental impacts which could, in turn, impact Lake Baikal (Borisova, 2019). Being an endorheic river delta, changes in water occurrence in this delta are not related to rising sea levels, but rather to hydroclimatic (Antokhina et al., 2019) and fluvial geomorphological processes (Pietron et al., 2018; Dong et al., 2018; Shinkareva et al., 2019). The anthropogenic impact on ecosystems in the Selenga River basin has increased in the recent decades, e.g., by the extraction of minerals, primarily gold, urbanization, and agricultural development, especially in the upper, Mongolian, part of the basin (Jarsjö et al., 2017; Garmaev et al., 2019). The long-term low water period observed in the region (Gelfan & Millionshchikova, 2018) has a significant impact on delta processes and wetland-dominated areas of the Selenga Delta (Ghajarnia et al., 2020), also posing drastic changes in sediment transport and water quality (Chalov et al., 2017b; Shinkareva et al., 2019).

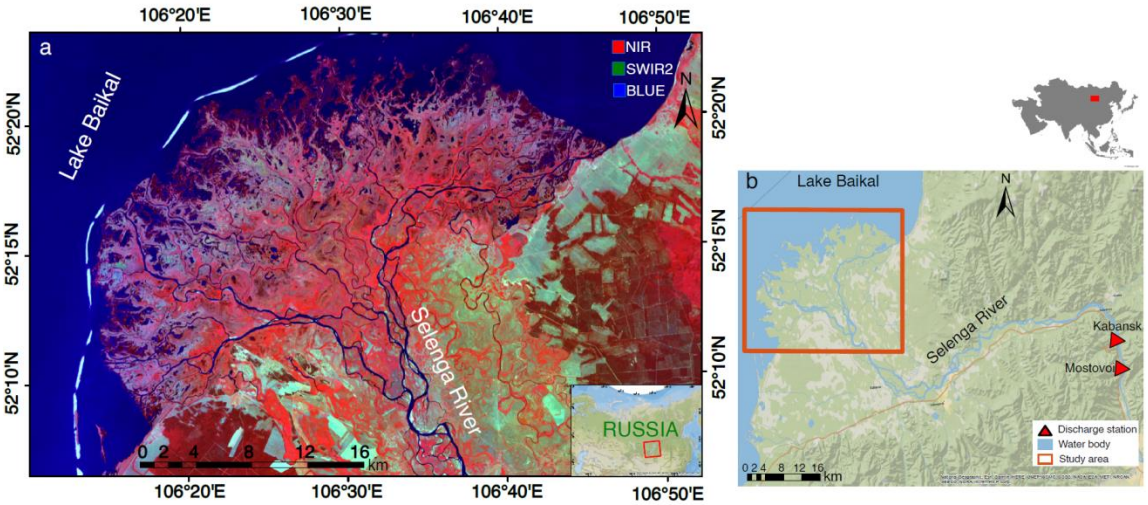

Figure 1. The Selenga River Delta. **a)** The location of the Selenga River Delta in Russia over a false-color Landsat 8 image acquired on 23 June 2017, path 132, frame 24. **b)** The location of the two discharge measuring stations used in this study (red triangles), roughly 100 km away from the Delta.

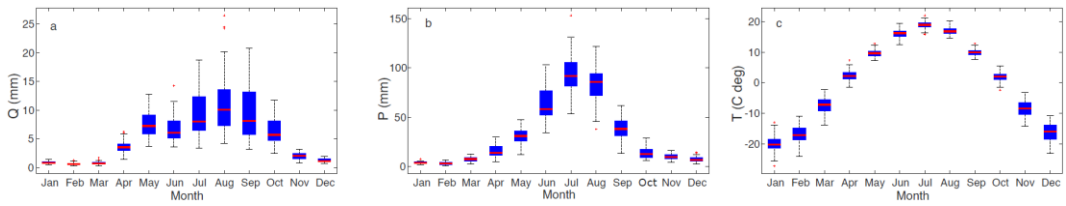

Figure 1. Mean runoff, precipitation, and temperature. Monthly box-whisker plots during the period 1985-2019 for **a)** Runoff (Q) in mm/month, **b)** precipitation (P) in mm/month, and **c)** temperature (T) in degrees centigrade. For the calculations of runoff, we divided discharge data at station Mostovoi by the upstream hydrological basin of 440,200 km^2, of which 67% falls in Mongolia and 33% in Russia.

2.2 Satellite data and classification

We mapped the occurrence of surface water in the Selenga River Delta in a time series of Landsat imagery. The classification data analyses were done using ENVI version 5.5 (Exelis Visual Information Solutions, Boulder, Colorado). We used Landsat Level-2 Surface Reflectance

data from the U.S. Geological Survey (Masek et al., 2006; Vermote et al., 2016, p. 8), which provides atmospherically corrected scenes of Landsat 4-5/TM, 7/ETM+, and 8/OLI upon request. In total, we obtained 195 images between 1987 and 2020 with less than 10% cloud cover over the scenes of the Selenga Delta but discarded more than half of the images due to Scan Line Corrector (SLC) errors (stripes on the Landsat-7 images due to instrument deficiency), cloud contamination, geometrical errors. Besides, several others acquired during winter were discarded since frozen water generates inaccurate classification results and unreliable water-land delineation. For the 87 remaining images, the Normalized Difference Vegetation Index (NDVI) and Normalized Difference Water Index (NDWI) were calculated by applying equation 1 and equation 2 (McFeeters, 1996), and stacked with Near Infrared (NIR), Shortwave Infrared (SWIR2) and the Blue band of each scene. The Red and Green represent the measured reflectance in the visible red band, and the visible green band of the spectrum, respectively. Since the highest reflectance difference between the water and the vegetation occurs in these bands and indices, using their combination in the classifier makes it possible to distinguish open water from the surrounding vegetation and land. Zhou et al. (2017) assessed the performance of different indices for differentiation of water surfaces and concluded that the NDWI-based algorithms (such as the one we used here) outperform other algorithms. However, classification methods might perform differently in different case studies (Zhou et al., 2017).

$$NDVI = \frac{NIR - Red}{NIR + Red} \quad Equation\ 1$$

$$NDWI = \frac{Green - NIR}{Green + NIR} \quad Equation\ 2$$

Before the supervised Maximum Likelihood classifier was applied on the stacked bands, we selected the training data of water surface recognition in each image by the visual inspection of the Google Earth's historical view on the corresponding date and the true-color composites of each scene (visible Red, Green, and Blue bands). We then applied the supervised Maximum Likelihood (ML) classifier on the stacked bands. The ML classification method is easy to

183 implement and has a fast processing procedure in comparison with other methods. The schematic
184 process is shown in Figure 3.

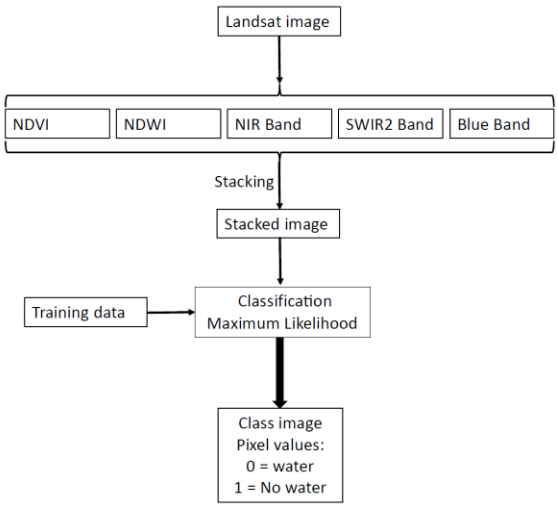

185

186 **Figure 2.** Schematic flowchart for the land-water delineation process

187

188 We tested the accuracy of the classification when using the mentioned band-index
189 combinations instead of only the available bands in Landsat products for fours specific Landsat
190 images and found that water surface classification is indeed improved (Tables S1 to S4,
191 Supplementary materials). Based on visual inspections, we prepared two sets of land-water data;
192 one for training the classifier and the other one for calculating the confusion Matrix and the
193 classification accuracy. To avoid misinterpretation, we chose the land-water data sets in similar
194 areas for all images as long as the delineation borders fitted the exact true-color locations of the
195 water bodies.

196 The Maximum Likelihood supervised classifier is widely applied to satellite imagery for
197 land cover mapping. Based on the training data, this algorithm assumes that the pixel classes are
198 normally distributed in the spectral space and calculates the probability of a pixel belonging to a
199 specific landcover class (c_m) (Richards, 1999) when the probability (p) of a pixel with a given
200 value (d) of belonging to c_m is higher than the probability of belonging to any other class c_n
201 (Richards, 1999) (equation 3).

202

$$d \in c_m \; if \; p(c_m|d) > p(c_n|d) \; for \; all \; n \neq m \quad Equation\ 3$$

203 2.3 Surface water occurrence and its changes

204 For each image and date, we classified each pixel binarily based on the results from the
205 supervised Maximum Likelihood classifier, either zero or one; representing the existence or non-
206 existence of surface water, respectively. Since only two classes are considered in the
207 calculations, the non-vegetation dry lands might be misclassified with the pixels identified as
208 water. To avoid this problem, we included the sand bars and other non-vegetation dry areas in
209 training data as much as possible. To be able to compare the water occurrence time series with
210 that of runoff from the main channel of the Selenga River and the lake levels of the Lake Baikal
211 we need a single value of water occurrence for each image. To get that value, we spatially
212 average the water occurrence of all pixels in a particular image. Therefore, we obtain the mean
213 water occurrence for each image ($\overline{w}_s$: subscript s represents the spatial mean) as:

$$\overline{w}_s = \frac{\sum_{i=1}^{r} v_{i,j}}{r} \quad Equation\ 4$$

214 where $v_{i,j}$ is the water occurrence of the i^{th} pixel in the class image j with the total number
215 of pixels r.

216 We followed a published methodology (Pekel et al., 2016) that estimates water
217 occurrence on a given land surface to quantify the occurrence of water in the Selenga River Delta
218 during the 33 years of the period 1987-2019. To obtain the water occurrence during the entire
219 33-year period, we calculated for each pixel the mean of the binary values of all images for that
220 specific pixel, leading to a final value between zero and one. Since not all months have the same
221 number of images available, our interpretation of water occurrence is more biased towards the
222 summer and autumn periods that contain more images due to favorable meteorological
223 conditions than the other seasons. To draw unbiased conclusions, we calculated a mean value of
224 water occurrence for each month in each pixel during the same period (w_m) as follows:

225

$$w_m = \frac{\sum_{j=1}^{n} v_{i,j}}{n} \quad Equation\ 5$$

where m is the month, j is a class image from the total of class images available for that specific month (n) from January 1987 to December 2019. While images taken in the summer and autumn periods have a higher quality and have a lower presence of clouds, images taken during the months of December, January, and February were discarded as the Lake Baikal and some parts of the Delta are covered by ice and snow, affecting the analysis of water occurrence. Moreover, we excluded the change in water occurrence of March since there is only one class image in March (located in the first period).

The mean water occurrence in each pixel and for the whole period ($\overline{w}$) is calculated by averaging the water occurrence of all months (w_m) as:

$$\overline{w} = \frac{\sum_{m=1}^{n=12} w_m}{12} \quad Equation\ 6$$

In order to understand the temporal change in water occurrence for each month of the year (Δw_m), we subtracted the mean w_m of the period 1987-2002 (w_{m1}) from that of the period 2003-2019 (w_{m2}) as:

$$\Delta w_m = w_{m2} - w_{m1} \quad Equation\ 7$$

Finally, the mean change of water occurrence ($\overline{\Delta w}$) per pixel was calculated by averaging the monthly changes of water occurrence Δw_m as:

$$\overline{\Delta w} = \frac{\sum_{m=1}^{n=12} \Delta w_m}{12} \quad Equation\ 8$$

As w_m ranges from zero to one, Δw_m and $\overline{\Delta w}$ do from -1 to +1, where a value of -1 means that the pixel did not contain water in any of the class images in the second period and contained water in all class images in the first period, and vice versa. Therefore, $\overline{\Delta w}$ provides information about the expansion and shrinkage of water surface area; the negative and positive values correspond to decreasing and increasing water occurrence, respectively. All of the raster calculations and visualizations were performed in the ArcGIS environment and MATLAB R2018a. Finally, we divided the Delta in three different regions of analysis (R1, R2, and R3,

respectively; Figure 4) to identify the two main drivers of water surface occurrence: 1) Oscillations of lake water level and 2) upstream water supply by main river discharge.

2.4 Hydroclimatic data and landcover map

We analyzed the dependence of surface water occurrence in the Delta on two hydrological variables: The Selenga River's surface runoff and water level in the Lake Baikal. For the first, we used daily discharge data from the Russian Federal Service for Hydrometeorology and Environmental Monitoring (Roshydromet) in the gauging stations closest to the Delta (Mostovoi and Kabansk stations), both located approximately 100 km upstream of the Delta. We also extracted temperature and precipitation data for the region of the Delta from the gridded data sets of the CRU of the Climatic Research Unit (Hulme, 1992; Hulme et al., 1998). Both data sets have 0.5° × 0.5° grids, with monthly data available from 1901 to 2018. For the case of precipitation, we used the mean monthly precipitation values of all cells fallen into the Selenga River basins upstream of each of the two discharge stations. To make surface water occurrence and runoff data comparable, we calculated the ten- and five-day averages of runoff data before, after, and on the acquisition date and time of the images.

For Lake Baikal water level, we used two gauge stations of the International Data Centre on Hydrology of Lakes and Reservoirs (Hydrolare) from 1963 to 2015, one roughly 60 km southwest of the Delta (coastal Babushkin station) and another one in the middle part of the Lake (Ushkanij station), together with the processed satellite altimetric data of the Hydroweb service (Crétaux et al., 2011) available since 1992 and continuously updated. The altimeters used in this dataset are Topex-Poseidon, Jason, Jason-2, Jason-3, and Sentinel-3A, and the point of observation is in the middle of the lake and near to the Ushkanij gauge station, which is roughly 200 km away from the Delta. Before 2014, the temporal resolution of this dataset was over ten days, and since 2014 new altimetric satellites have been launched in the orbits, giving one-day resolution water level data.

We further studied water occurrence and its changes in the different land cover ecosystems present in the Delta, such as permanent water bodies, seasonally inundated areas, and lands, wetlands, and forests (Figure 4). We preliminarily assigned a landcover category to each pixel based on their $\overline{w}$ values; pixels with $\overline{w} > 80\%$ falling into the permanent water category, pixels with $\overline{w} < 10\%$ into dry lands and between $10\% < \overline{w} < 80\%$ as seasonal water bodies. We

merged this preliminary water occurrence categorization with the dynamic land cover map of the Copernicus Global Land Service at 100-m resolution (CGLS-LC100) (Buchhorn et al., 2019) (Fig. 4). This product, obtained via Google Earth Engine, has global coverage and its reference year is 2015.

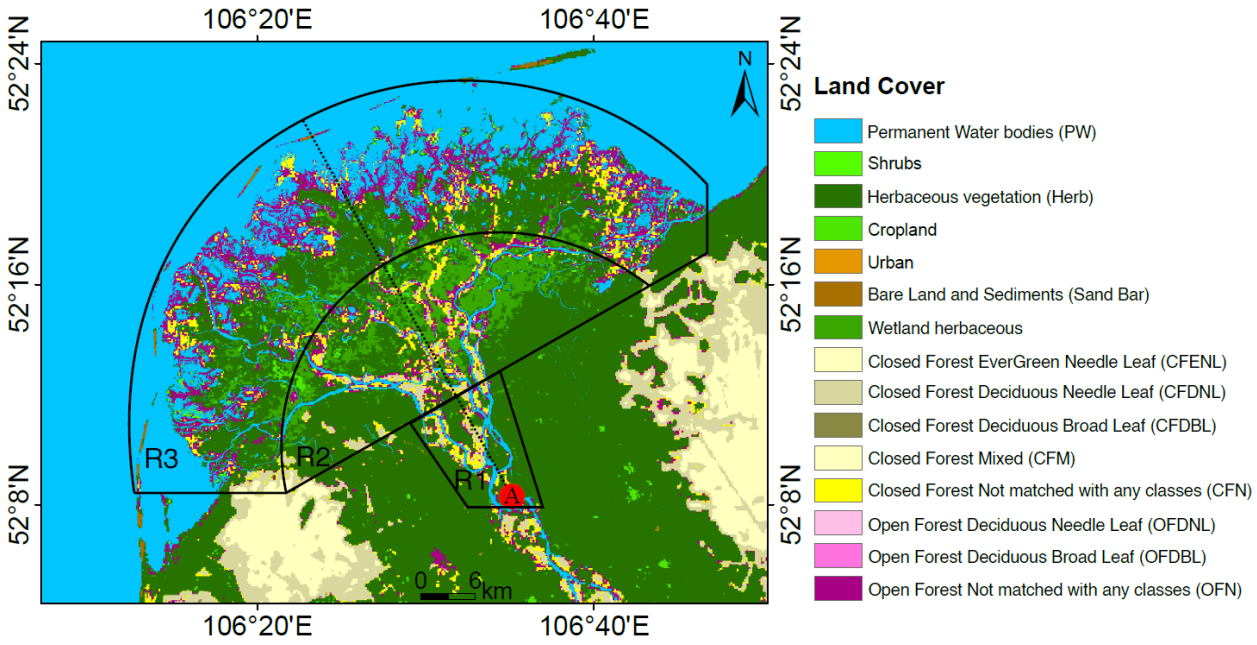

Figure 3. Land cover (CGLS-LC100) and three regions of focus in the Delta. The closest upstream borders of R2 and R3 are 10- and 20-km downstream from point A along the dashed line, respectively.

3 Results

Precipitation and runoff in the Selenga River Basin (area = 445,000 km^2) have decreased during the period 1987-2019, with a consistent drop from the highest reported peak in 1992 to its lowest been 2004 and 2008. Air temperature in the Delta increased to the highest mean annual values in 2016 and 2017 (Figure 5). The map of mean water occurrence $\overline{w}$ (Figure 6) visualizes the stream network and the areas susceptible to seasonal flooding. As expected, areas along the coast of the Lake Baikal have a higher water occurrence than those inland. The change in water occurrence between the two periods $\overline{\Delta w}$ (Figure 7) shows the expansion and shrinkage of the surface water areas attributed to river planform migration, newly formed or dried out streams and lakes, and the flooding of flood-prone areas. The supplementary table S5 shows the number of images per month and year used to produce the map of water occurrence and its changes. In

general, negative values of $\overline{\Delta w}$ (red in Figure 7) are dominant across the Delta and concentrated in the southwest and eastern sections, where the water extent has mostly decreased.

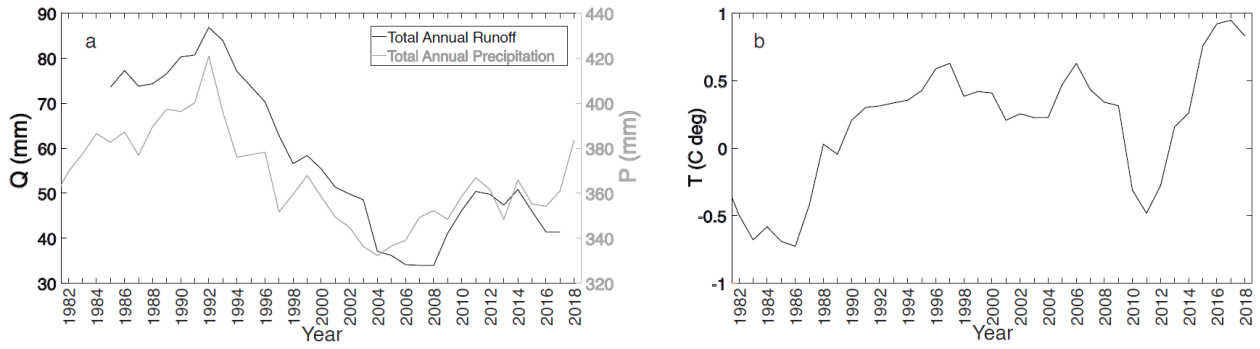

Figure 4. The time series of Runoff (Q), Precipitation (P), and Temperature (T) in the Selenga River hydrological basin. a) the 5-year moving average of total annual P on the right axis and Q on the left axis. **b)** the 5-year moving average of T.

A first look into the spatial distribution of $\overline{\Delta w}$ highlights a decreased water occurrence in the outer sediment banks in the proximity of Lake Baikal due to the accumulation of sediments and a decline in coverage of surface water (Figure 7). Decreasing $\overline{\Delta w}$ in close vicinity of the main channel and streams' bends shows instead river planform migration as sand and grabble areas are uncovered. Water occurrence $\overline{w}$ shows for example two possible paths of a river branch (e.g., panel m1 in Figures 6 and 7). The availability of the images does not allow to determine the specific day when the change in river course took place; however, the class images available between 1999 and 2001 show the traces of the newly-formed path. Additionally, the change Δw hints which is the old (north-eastern direction) and new (north-western direction) path, due to changes in water occurrence. The same analysis in panel m2 points instead to the presence of river bends and temporary water bodies, in which $\overline{w}$ is still high but less than that of permanent water bodies. Also, when $\overline{\Delta w}$ is high (close to -1 or +1) it shows where in the river network are meandering processes occurring and when can these lead to oxbow lake formation in the future.

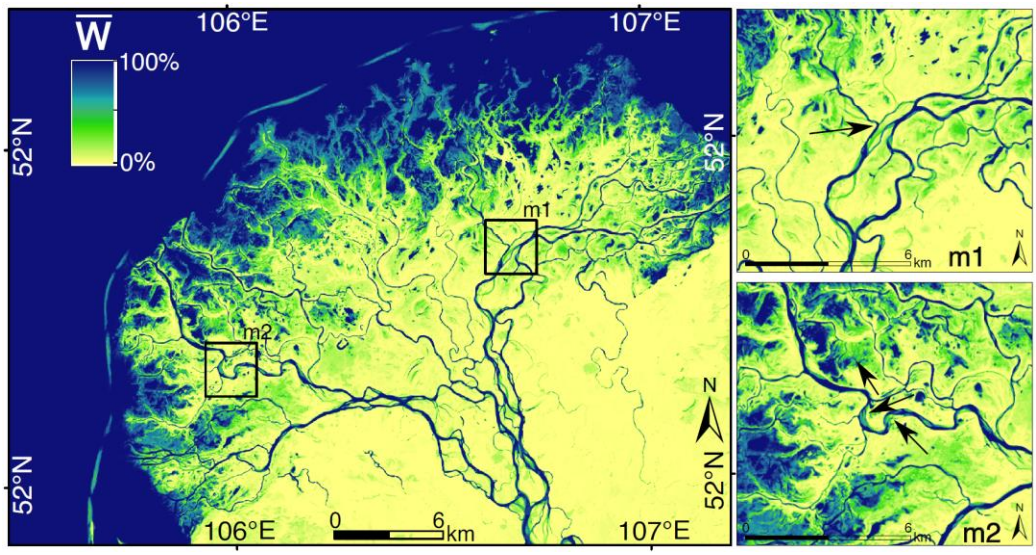

Figure 6. Mean Surface water occurrence ($\bar{w}$) in 1987–2019. Pixels not holding water in any of the class images are in yellow (0%) and pixels that hold water in all class images in dark blue (100%). The arrow in zoom panel m1 shows a change in river course. The arrows in zoom panel m2 show river bends and flood-prone areas with high water occurrence but still less than that of permanent water bodies.

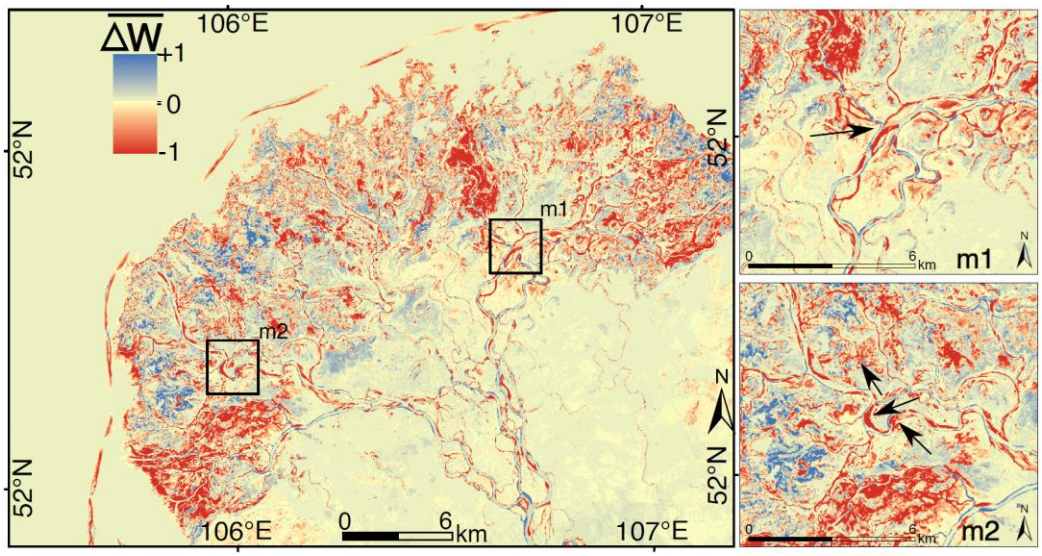

Figure 7. Change in surface water occurrence ($\overline{\Delta w}$) between 1987-2002 and 2003-2019. Red areas (-1) show loss of water surface and blue areas a gain (+1).

Based on the CGLS-LC100 landcover map shown in Figure 4, we summarized the distribution of $\bar{w}$ and $\overline{\Delta w}$ for each landcover (Figure 8 and Figure 9a). In general, there is a decrease in water occurrence throughout the Delta. The decrease in water occurrence is more recurrent in seasonally flooded areas and even larger than the decrease in permanent water bodies (Figure 9.b). By dividing the number of pixels in which the water occurrence has changed by the total number of pixels available in each category, we show that the mean water occurrence in the permanent water bodies changed only in 20% of the pixels, while in seasonally flooded water it did in 90% of the pixels. The number of pixels is presented in the supplementary table S6.

In the permanent water bodies of the river channel, $\overline{\Delta w}$ varies between -0.17 and +0.08, with the increasing water occurrence located near the river bends (green colors in Figure 6). Although $\bar{w}$ in the outer bank of the Delta (the sand bar near the Lake) is larger than 60%, the negative values of $\overline{\Delta w}$ confirm a decrease in water occurrence as the sand bars have become thicker during the last three decades. The $\bar{w}$ in closed and open forests with needle-leaf trees (CFDNL and OFDNL) and perennial woody crops is less than 10% and is fairly constant. However, due to the canopy coverage in these regions and the limitations of Landsat products, it is not always possible to monitor the surface water beneath the tree canopy. The largest values of $\bar{w}$ are found in areas covered by herbaceous vegetation (Herb) and shrubs (the plants that are less than five meters tall) such as the wetland-dominated areas and in the proximity of the river network, as they are more susceptible to river overflow (Figure 9a). Although in areas covered by shrubs, the water occurs in more than 60% of the images, there is a general shrinkage of the water surface in the majority of the pixels in these land covers (Figure 9a). Although this implies that these areas are flooded less frequently in the second period than they were in the first period, we cannot rule out the cause of an increase in the vegetation canopy due to the sensibility of Landsat products to vegetation growth.

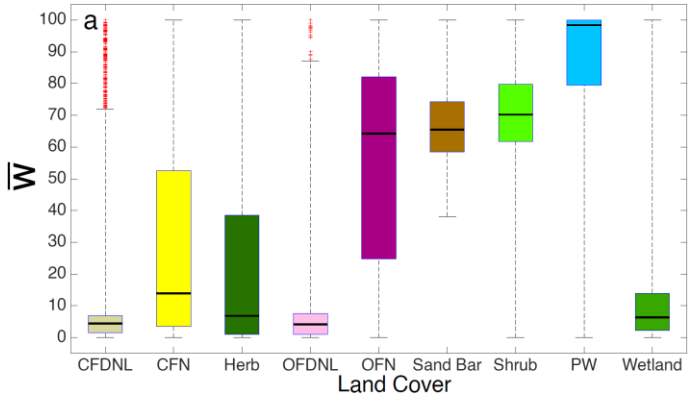

Figure 8. The distribution of $\overline{w}$ for each land cover, with colors and acronyms corresponding to Figure 4.

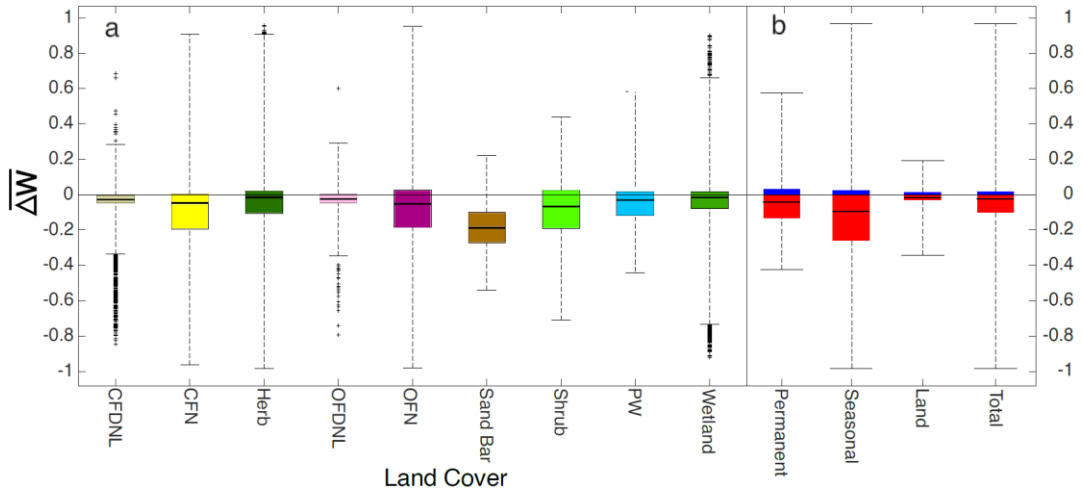

Figure 9. The distribution of $\overline{\Delta w}$ **a)** for each land cover and **b)** permanent water, seasonal water, and land categories.

Supplementary Figure S1 shows the scatter plot of the monthly average of NDVI versus the monthly average of water occurrence and it can be seen that a significant linear regression exists between these two parameters. Thus, by increasing NDVI in the growing season (June to August) the water occurrence decreases.

3.1 Relation of water occurrence to runoff and water level in Lake Baikal

The distributions of mean change in monthly water occurrence Δw_m between the periods 1987-2002 and 2003-2019 for all the pixels (where $\Delta w_m \neq 0$) within the total area of the Selenga River Delta (i.e., R1+R2+R3) are shown in Figure 10 along with the change in monthly

runoff (ΔQ) in station Kabansk. The $\bar{w}$ has mostly decreased in all months but October, as the median of the Δw_m the distributions are negative, agreeing with a generic decrease in runoff throughout all months and most notorious in August. Runoff instead has decreased the most in the month of august. Interestingly, the month of October sees the greatest number of pixels showing an increase in w_m, while the following month, November, sees the second smallest decrease in Q.

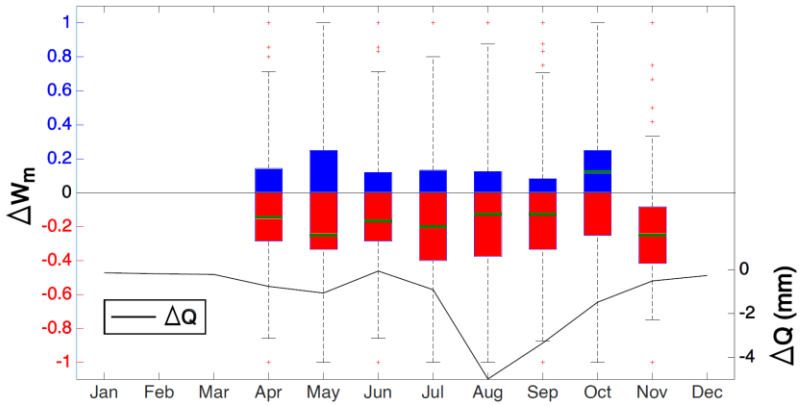

Figure 10. Monthly distributions of change in water occurrence (Δw_m) and runoff (ΔQ) between the periods 1987-2002 and 2003-2019 for the area of the Selenga River Delta (R1, R2, and R3).

In order to determine if changes in water occurrence $\bar{w}_s$ in the Selenga River Delta were more related to changes in the lake or the river, we calculated the R^2 and statistical significance value ($p < 0.05$; Pearson) of the linear regression between $\bar{w}_s$ and Q (and water level (WL) in the lake). We find a positive and significant ($p < 0.05$) linear regression between Q and $\bar{w}_s$ that is significant in all three regions and highest (R^2=0.58) in the mid-region R2. The most relevant changes in water occurrence in the Delta seem to also replicate those in the Q series of the Selenga River, for example, the peaks of 1995, 1998, and 2014, after applying a LOESS filter to the time series (locally estimated scatterplot smoothing), as data points are not spread unfirmly in time due to image availability (Figure 11a). This result is found regardless of the discharge station selected and different temporal moving windows of Q (i.e., instantaneous and 5-day and 10-day averages of Q before and after the images' acquisition dates). In contrast, the lake water level does not influence the water occurrence of the class images, as all R^2 values are very low,

391 signaling a low influence of the backwater effect of the Lake on water occurrence in the Delta
392 (Figure 11b, S2-S3).

393 **Table 1**

394 *Linear Regression Between $\overline{w}_s$ and I) Runoff (Q) and II) Water Level (WL) in Lake Baikal, for*
395 *Three Regions R1, R2 and R3.*

396

	$\overline{w}_s$ vs. Q		$\overline{w}_s$ vs. WL (Altimetry)	
	R^2	p-value	R^2	p-value
Region 1	0.213	3.13e-05	0.0026	0.644
Region 2	***0.58***	2.22e-15	***0.0591***	0.0268
Region 3	0.0791	0.0145	0.0004	0.864
Entire Delta	0.0222	0.202	0.0028	0.635

397

398 *Note.* Bold values are the highest of all regions. The surface runoff data are selected on
399 the images' acquisition days, and the Lake water levels are nearest to the date of acquisitions.

400

401

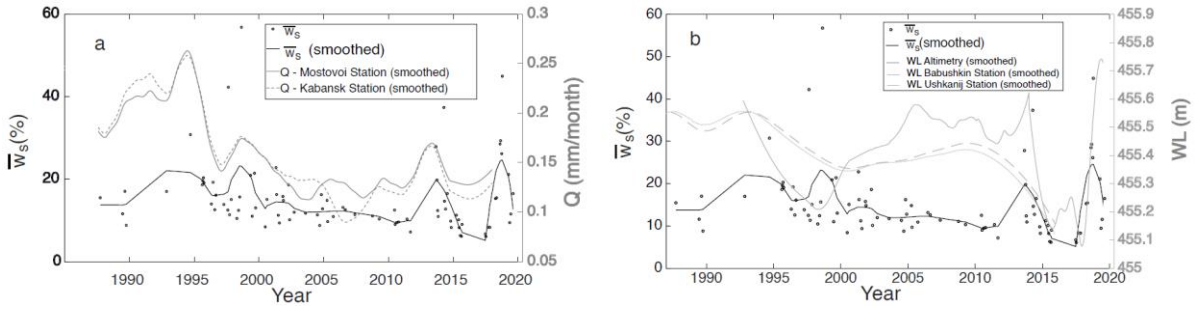

402

403 **Figure 11.** The relationship between $\overline{w}_s$ (left vertical axis) and **a)** Q and **b)** Water Level in Lake
404 Baikal in region R2 (right vertical axis). Lines represent a Loess filter. The surface of reference

for the gauge stations is the sea level and for the altimetric water levels is geoid GGMO2C (Tapley et al., 2005).

4 Discussion

We have found a net decrease in surface water occurrence in the Selenga River Delta within the period 1987-2019 which agrees with a recent finding of a general decrease in water occurrence in Norther Siberia (Borja et al., 2020), with both permanent and seasonal flooded areas considered in both studies. Borja et al. (2020) also found that most decreases in surface water area occurred in areas of seasonal flooding due to decreasing discharge in the rivers after 1997. On the other hand, studies that have not considered seasonally flooded areas show different magnitude of changes in water occurrence. Pekel et al. (2016) and Donchyts et al. (2016) found a global net increase in water occurrence, but the latter found a smaller expansion of water surface than the former by taking into account only permanent water bodies (Borja et al., 2020; Donchyts et al., 2016; Pekel et al., 2016).

Moreover, different periods of analysis yield different results of changes in water occurrence. For example, Borja et al. (2020) showed that two periods of 1985-2000 vs 2001-2015 and 1985-2005 vs 2013-2015 led to different magnitudes of a global increase in water occurrence while Pekel et al. (2016) and Donchyts et al. (2016) studied the periods of 1985-1997 vs 1998-2005 and 1985-2005 vs 2013-2015, respectively, to find different magnitudes of increased water occurrence.

We find in the case of the Selenga River Delta, that changes in water occurrence are more related to changes in upstream runoff (R^2=0.58) rather than changes in water level in the lake (R^2=0.05). This is probably due to the water budget in the Delta arising from the variability of discharge, as water enters the delta, is temporarily stored within its boundaries to be later discharged into Lake Baikal. In addition, the Selenga River has not been regulated by flow divergence or dam construction. Other unregulated deltas and upstream rivers have also shown high correlations between changes in water level and upstream discharge (Palomino-Ángel et al., 2019). On the contrary, Jaramillo et al. (2018) found that in the case of the Magdalena River Delta in Colombia, the relationship between water level change and change in upstream river discharge was much lower (R^2=0.17) due to the regulation of freshwater into the Delta.

The relationship between water occurrence and upstream runoff should be theoretically higher, as the Selenga River is the only freshwater input into the Delta. More water discharge brings more sediment loads, that when accumulated, leading to a gain in dry surfaces. It is known that the Delta retains ~3000 tons/day of suspended sediments, an amount that outweighs the total flux of sediments to the entire Lake (Chalov et al., 2015). However, this may not be the case for the Selenga River delta under the period of study. Chalov et al. (2015) found that during the period 1983-2011 the correlation factor between the surface runoff and the suspended sediment concentration was only 0.16 (Chalov et al., 2015; Moragoda & Cohen, 2020). Furthermore, no significant overbank flow has been observed in the flood season after 2011 (Chalov et al., 2015), leading to no flooding from bank overflow, reducing an even stronger relationship between discharge and water occurrence.

On the other hand, the weak relationship between water occurrence and water level in Lake Baikal is due to the fact that water levels of Lake Baikal are currently regulated by the Irkutsk dam on the main outflow of Lake Baikal – Angara River. Since the Irkutsk dam was created in 1959, lake water levels are more homogeneous than before (during the last three decades are within half a meter), and such changes may not imply considerable changes in water occurrence in the Delta.

The results of a study published in 2020 indicate that 1000 deltas show a net land gain of 54 ± 12 km^2 per year (Nienhuis et al., 2020). Although the deltas studied herein are wave, tide, and river-dominated and are affected by the sea-level rise, the authors showed that deforestation is responsible for such gain of land area in the Deltas. In the case of the Selenga River Delta, a decrease in water occurrence (water surface shrinkage) intensifies the effect of the land gain.

Our results also show that the change in water occurrence is not heterogeneous throughout the Delta. The spatial percentage of the shrinkage of the water surface (in the R2 region) in the left, right, and the middle part of the Delta is 44%, 51%, and 52%, respectively. These results are consistent with the findings in Chalov et al., (2017a) that show the maximum lift between 1956 and 1998 happened in the right and the middle side of the Delta, and more recently some water bodies are filled with sediment that contributed to the growth of the Delta. Their estimation shows higher relative suspended sediment retention in the middle and the right side of the Delta (Chalov et al., 2017a). Although the sediment discharge is decreasing in the

area, the surface of the Delta is rising by a velocity of 75 cm/year (Chalov et al., 2017a). In terms of the longitudinal change of the water occurrence, the spatial percentage of the water loss in regions R1(River bifurcation), R2(wetland-dominated area), and R3 (closer to the Lake) are 0.41%, 0.49%, and 45% respectively. These results show that wetland-dominated areas with low elevations are more influenced by river and lake water levels.

5 Conclusions

The spatial distribution of changes in water surface in the Selenga River Delta relate to inputs of freshwater and sediment into the Delta, which are important for the urban, agricultural, and industrial use, and the ecology of the Delta. We find that:

1. The mean water occurrence in the Selenga River Delta decreased between 1987-2002 and 2003-2019. The decreasing water occurrence is mostly in seasonally flooded regions rather than in permanent water bodies. The outer bank of the Delta, the border of the Lake and the Delta, have gained land probably by sediment accumulation. The largest changes in water occurrence are mostly seen along the mainstream bends due to planform migration, and highlighted by the case of a change in direction of the river course in the east of the Delta.

2. There is a significant relationship between water occurrence and the surface runoff. The best fit between these two parameters was observed for the inner zone of the Delta with an R^2 of 0.58. On the contrary, water occurrence does not correlate with the Lake water level.

3. We have improved the common methodology of determining water occurrence by providing the training data for all of the available images in Maximum Likelihood supervised classification.

The change in water occurrence between 1987-2002 and 2003-2019 shows that river planforms, stream networks, and consequently the shape of the Delta are changing due to changes in river discharge. We expect that any modification of the river flow through upstream damming and water diversion compounded by climate change will significantly impact the Selenga River Delta.

6 Acknowledgements and Data Accessibility

The project was funded by Swedish Research Council for Environment, Agricultural Sciences and Spatial Planning FORMAS (942–2015-740), and the Swedish National Space Agency (180/18).

SCH was supported by Russian Fund for Basic research project 18-05-80094 and 19-05-50109.

The Landsat Level-2 Surface Reflectance data were obtained from the U.S. Geological Survey (https://earthexplorer.usgs.gov/) and are freely available On-demand. They are described in these citation references: Masek et al. (2006), Vermote et al. (2016), p. 8. Digital Object Identifier (DOI) for L8, L7 and L4 data respectively: [https://doi.org/10.5066/F78S4MZJ], [https://doi.org/10.5066/F7Q52MNK], [https://doi.org/10.5066/F7KD1VZ9].

The temperature and precipitation data for the region of the delta were obtained from the gridded data sets of the CRU of the Climatic Research Unit and are available in these in-text data citation references: Hulme (1992) [with Open Database License: http://opendatacommons.org/licenses/odbl/1.0/ and Database Contents License: http://opendatacommons.org/licenses/dbcl/1.0/ under conditions of Attribution and Share-Alike: http://opendatacommons.org/licenses/odbl/summary/], Hulme et al. (1998).

The dynamic land cover map of the Copernicus Global Land Service at 100-m resolution (CGLS-LC100) is available at this in-text citation reference: Buchhorn et al. 2019.

For Lake Baikal water level, we used two gauge stations of the International Data Centre on Hydrology of Lakes and Reservoirs (Hydrolare) from 1963 to 2015, Babushkin station and Ushkanij station, together with the processed satellite altimetric data of the Hydroweb service (Crétaux et al., 2011) available since 1992 and continuously updated.

The daily discharge data were obtained from the Russian Federal Service for Hydrometeorology and Environmental Monitoring (Roshydromet) in the gauging stations closest to the Delta (Mostovoi and Kabansk stations) and are not accessible to the public or research community.

References

Allen, G. H., & Pavelsky, T. M. (2018). Global extent of rivers and streams. *Science*, *361*(6402), 585–588. https://doi.org/10.1126/science.aat0636

Antokhina, O.Y., Latysheva, I.V., Mordvinov, V.I. (2019). A case study of Mongolian Cyclogenesis during the July 2018 blocking events. Geogr. Environ. Sustain. *Geography, Environment, Sustainability*, 12(3), pp.66-78. https://doi.org/10.24057/2071-9388-2019-14

Berhane, T. M., Lane, C. R., Wu, Q., Autrey, B. C., Anenkhonov, O. A., Chepinoga, V. V., & Liu, H. (2018). Decision-tree, rule-based, and random forest classification of high-resolution multispectral imagery for wetland mapping and inventory. *Remote Sensing*, *10*(4), 580. https://doi.org/10.3390/rs10040580

Borisova, T. A. (2019). The evaluation of natural risks of floods in the Delta of the River Selenga and engineering protection against flooding. In *IOP Conference Series: Earth and Environmental Science* (Vol. 272, p. 022232). https://doi.org/doi:10.1088/1755-1315/272/2/022232

Borja, S., Kalantari, Z., & Destouni, G. (2020). Global wetting by seasonal surface water over the last decades. *Earth's Future*, *8*(3), e2019EF001449. https://doi.org/10.1029/2019EF001449

Buchhorn, M., Smets, B., Bertels, L., Lesiv, M., Tsendbazar, N. E., Herold, M., & Fritz, S. (2019). Copernicus global land service: Land Cover 100m: Epoch 2015: Globe. *Version V2. 0.2*. https://doi.org/10.5281/zenodo.3243509

Chalov, S., Jarsjö, J., Kasimov, N. S., O. Romanchenko, A., Pietroń, J., Thorslund, J., & Promakhova, E. V. (2015). Spatio-temporal variation of sediment transport in the Selenga River Basin, Mongolia and Russia. *Environmental Earth Sciences*, *73*(2), 663–680. https://doi.org/10.1007/s12665-014-3106-z

Chalov, S., Thorslund, J., Kasimov, N., Aybullatov, D., Ilyicheva, E., Karthe, D., et al. (2017a). The Selenga River Delta: A geochemical barrier protecting Lake Baikal waters. *Regional Environmental Change*, *17*(7), 2039–2053. https://doi.org/10.1007/s10113-016-0996-1

Chalov, S., Bazilova, V., Tarasov, M. (2017b). Suspended sediment balance in Selenga Delta at the Late XX–Early XXI Century: Simulation by LANDSAT satellite smages. *Water Resources* Vol. 44, No. 3, pp. 463–470. https://doi.org/10.1134/S0097807817030071

Chini, M., Hostache, R., Giustarini, L., & Matgen, P. (2017). A hierarchical split-based approach for parametric thresholding of SAR images: Flood inundation as a test case. *IEEE Transactions on Geoscience and Remote Sensing*, *55*(12), 6975–6988. https://doi.org/10.1109/TGRS.2017.2737664

Crétaux, J.-F., Jelinski, W., Calmant, S., Kouraev, A., Vuglinski, V., Bergé-Nguyen, M., et al. (2011). SOLS: A lake database to monitor in the Near Real Time water level and storage variations from remote sensing data. *Advances in Space Research*, *47*(9), 1497–1507. https://doi.org/10.1016/j.asr.2011.01.004

Cui, Y., Xiao, R., Zhang, M., Wang, C., Ma, Z., Xiu, Y., Wang, Q. and Guo, Y. (2020). Hydrological connectivity dynamics and conservation priorities for surface-water patches in the Yellow River Delta National Nature Reserve, China. *Ecohydrology & Hydrobiology*. https://doi.org/10.1016/j.ecohyd.2020.03.005

Donchyts, G., Baart, F., Winsemius, H., Gorelick, N., Kwadijk, J., & Van De Giesen, N. (2016). Earth's surface water change over the past 30 years. *Nature Climate Change*, *6*(9), 810–813. https://doi.org/10.1038/nclimate3111

Dong, T. Y., Nittrouer, J. A., Czapiga, M. J., Ma, H., McElroy, B., Il'icheva, E, Pavlov M, Chalov S, Parker G. (2019). Roles of bank material in setting bankfull hydraulic geometry as informed by the Selenga River delta, Russia. *Water Resources Research* Volume 55, Issue 1, pp. 827-846. https://doi.org/10.1029/2017WR021985

Garmaev, E.Z., Kulikov, A.I., Tsydypov, B.Z., Sodnomov, B. V., Ayurzhanaev, A.A. (2019). Environmental conditions of Zakamensk Town (Dzhida River Basin Hotspot). *Geography, Environment, Sustainability*, 12(3), pp.224-239. https://doi.org/10.24057/2071-9388-2019-32

Gelfan, A.N., Millionshchikova, T.D. (2018). Validation of a hydrological model intended for impact study: Problem statement and solution example for Selenga River Basin. *Water Resources*, 45, 90–101. https://doi.org/10.1134/S0097807818050354

Ghajarnia, N., Destouni, G., Thorslund, J., Kalantari, Z., Åhlén, I., Anaya-Acevedo, J.A., Blanco-Libreros, J.F., Borja, S., Chalov, S., Chun, K.P., Desormeaux, A., Garfield, B.,

Hansen, A., Jaramillo, F., Jarsjö, J., Labbaci, A., Livsey, J., Maneas, G., McCurley, K., Palomino-Ángel, S., Pietron, J., Price, R., Monroy, V.R., Salgado, J., Sannel, B., Seifollahi-Aghmiuni, S., Sjöberg, Y., Tersky, P., Vigouroux, G., Villanueva, L.L. (2020). Data for wetlandscapes and their changes around the world. *Earth System Science Data*, 12(2), pp.1083-1083. https://doi.org/10.5194/essd-12-1083-2020

Giesen, N. van de. (2020). Human activities have changed the shapes of river deltas. *Nature*, *577*(7791), 473–474. https://doi.org/10.1038/d41586-020-00047-y

Golden, H. E., Lane, C. R., Amatya, D. M., Bandilla, K. W., Raanan Kiperwas, H., Knightes, C. D., & Ssegane, H. (2014). Hydrologic connectivity between geographically isolated wetlands and surface water systems: A review of select modeling methods. *Environmental Modelling & Software*, *53*, 190–206. https://doi.org/10.1016/j.envsoft.2013.12.004

Guo, M., Li, J., Sheng, C., Xu, J., & Wu, L. (2017). A review of wetland remote sensing. *Sensors*, *17*(4), 777. https://doi.org/10.3390/s17040777

Hulme, M. (1992). A 1951–80 global land precipitation climatology for the evaluation of general circulation models. *Climate Dynamics*, *7*(2), 57–72. https://doi.org/10.1007/BF00209609

Hulme, M., Osborn, T. J., & Johns, T. C. (1998). Precipitation sensitivity to global warming: Comparison of observations with HadCM2 simulations. *Geophysical Research Letters*, *25*(17), 3379–3382. https://doi.org/10.1029/98GL02562

Jaramillo, F., Brown, I., Castellazzi, P., Espinosa, L., Guittard, A., Hong, S.-H., et al. (2018). Assessment of hydrologic connectivity in an ungauged wetland with InSAR observations. *Environmental Research Letters*, *13*(2), 024003. https://doi.org/10.1088/1748-9326/aa9d23

Jarsjö J, Chalov S, Pietroń J, Alekseenko A, Thorslund J. (2017). Patterns of soil contamination, erosion, and river loading of metals in a gold mining region of Northern Mongolia. *Regional Environmental Change*, 17(7): 1991-2005. https://doi.org/10.1007/s10113-017-1169-6

Lane, C. R., Liu, H., Autrey, B. C., Anenkhonov, O. A., Chepinoga, V. V., & Wu, Q. (2014). Improved wetland classification using eight-band high resolution satellite imagery and a hybrid approach. *Remote Sensing*, *6*(12), 12187–12216. https://doi.org/10.3390/rs61212187

608 Lane, C. R., Anenkhonov, O., Liu, H., Autrey, B. C., & Chepinoga, V. (2015). Classification and
609 inventory of freshwater wetlands and aquatic habitats in the Selenga River Delta of Lake
610 Baikal, Russia, using high-resolution satellite imagery. *Wetlands Ecology and*
611 *Management*, *23*(2), 195–214. https://doi.org/10.1007/s11273-014-9369-z
612 Lu, Z., & Kwoun, O. i. (2008). Radarsat-1 and ERS InSAR analysis over Southeastern coastal
613 Louisiana: Implications for mapping water-level changes beneath swamp forests. *IEEE*
614 *Transactions on Geoscience and Remote Sensing*, *46*(8), 2167–2184.
615 https://doi.org/10.1109/TGRS.2008.917271
616 Masek, J. G., Vermote, E. F., Saleous, N. E., Wolfe, R., Hall, F. G., Huemmrich, K. F., et al.
617 (2006). A Landsat surface reflectance dataset for North America, 1990-2000. *IEEE*
618 *Geoscience and Remote Sensing Letters*, *3*(1), 68–72.
619 https://doi.org/10.1109/LGRS.2005.857030
620 McFeeters, S. K. (1996). The use of the Normalized Difference Water Index (NDWI) in the
621 delineation of open water features. *International Journal of Remote Sensing*, *17*(7),
622 1425–1432. https://doi.org/10.1080/01431169608948714
623 Moragoda, N., & Cohen, S. (2020). Climate-induced trends in global riverine water discharge
624 and suspended sediment dynamics in the 21st century. *Global and Planetary Change*,
625 *191*, 103199. https://doi.org/10.1016/j.gloplacha.2020.103199
626 Nguyen Thanh, T., Tri, V.P.D., Kim, S., Phuong, T.N., Mong, T.L. and Tuan, P.V. (2020). A
627 subregional model of system dynamics research on surface water resource assessment for
628 paddy rice production under climate change in the Vietnamese Mekong Delta. *Climate*,
629 8(3), p.41. https://doi.org/10.3390/cli8030041
630 Nienhuis, J. H., Ashton, A. D., Edmonds, D. A., Hoitink, A. J. F., Kettner, A. J., Rowland, J. C.,
631 & Törnqvist, T. E. (2020). Global-scale human impact on delta morphology has led to net
632 land area gain. *Nature*, *577*(7791), 514–518. https://doi.org/10.1038/s41586-019-1905-9
633 Palomino-Ángel, S., Anaya-Acevedo, J.A., Simard, M., Liao, T.H. and Jaramillo, F. (2019).
634 Analysis of floodplain dynamics in the Atrato River Colombia using SAR
635 interferometry. *Water*, 11(5), p.875. https://doi.org/10.3390/w11050875
636 Pekel, J.-F., Cottam, A., Gorelick, N., & Belward, A. S. (2016). High-resolution mapping of
637 global surface water and its long-term changes. *Nature*, 540(7633), 418.
638 https://doi.org/10.1038/nature20584

639 Pietroń, J., Nittrouer, J.A., Chalov, S.R.; Dong, T.Y., Kasimov, N., Shinkareva, G., Jarsjö, J.
640 (2018). Sedimentation patterns in the Selenga River Delta under changing hydroclimatic
641 conditions. *Hydrological processes*, 32(2), pp.278-292.
642 https://doi.org/10.1002/hyp.11414
643 Potemkina, T. G. (2011). Sediment runoff formation trends of major tributaries of Lake Baikal in
644 the 20th century and at the beginning of the 21st century. *Russian Meteorology and*
645 *Hydrology*, *36*(12), 819–825. https://doi.org/10.3103/S1068373911120077
646 Richards, J. A. (1999). Remote sensing digital image analysis (Vol. 3). Springer. Retrieved from
647 DOI 10.1007/978-3-642-30062-2
648 Shinkareva G.L., Lychagin M.Y., Tarasov M.K., Pietroń J., Chichaeva M.A., Chalov S.R.
649 (2019). Biogeochemical specialization of macrophytes and their role as a biofilter in the
650 Selenga Delta. *Geography, Environment, Sustainability*, 10, pp.2071-9388.
651 https://doi.org/10.24057/2071-9388-2019-103
652 Syvitski, J. P., Kettner, A. J., Overeem, I., Hutton, E. W., Hannon, M. T., Brakenridge, G. R., et
653 al. (2009). Sinking deltas due to human activities. *Nature Geoscience*, *2*(10), 681–686.
654 https://doi.org/10.1038/ngeo629
655 Tapley, B., Ries, J., Bettadpur, S., Chambers, D., Cheng, M., Condi, F., Gunter, B., Kang, Z.,
656 Nagel, P., Pastor, R. and Pekker, T. (2005). GGM02–An improved Earth gravity field
657 model from GRACE. *Journal of Geodesy*, 79(8), pp.467-478. DOI 10.1007/s00190-005-
658 0480-z
659 Vermote, E., Justice, C., Claverie, M., & Franch, B. (2016). Preliminary analysis of the
660 performance of the Landsat 8/OLI land surface reflectance product. *Remote Sensing of*
661 *Environment*, *185*, 46–56. https://doi.org/10.1016/j.rse.2016.04.008
662 Zhang, G., Yao, T., Piao, S., Bolch, T., Xie, H., Chen, D., et al. (2017). Extensive and drastically
663 different alpine lake changes on Asia's high plateaus during the past four decades.
664 *Geophysical Research Letters*, *44*(1), 252–260. https://doi.org/10.1002/2016GL072033
665 Zhou, Y., Dong, J., Xiao, X., Xiao, T., Yang, Z., Zhao, G., et al. (2017). Open surface water
666 mapping algorithms: A comparison of water-related spectral indices and sensors. *Water*,
667 *9*(4), 256. https://doi.org/10.3390/w9040256

668

669